28. J. Korenaga, S. Karato, *J. Geophys. Res.* **113**, B02403 (2008).
29. S. C. Solomon, R. P. Comer, J. W. Head, *J. Geophys. Res.* **87**, 3975 (1982).
30. Dislocation creep of olivine is assumed to be the dominant deformation process in the mantle.
31. H. J. Melosh, *Impact Cratering: A Geologic Process* (Oxford Univ. Press, Oxford, 1989).
32. A. C. Cook, T. R. Watters, M. S. Robinson, P. D. Spudis, *J. Geophys. Res.* **105**, 12023 (2000).
33. R. J. Pike, *Proc. Lunar Planet. Sci. Conf.* **8**, 3427 (1977).
34. We thank the engineers of NEC/Toshiba Space Systems Ltd., Nippon Antenna Co. Ltd., and Japan Aircraft Mfg. Co. Ltd. and the entire staff of the SELENE mission, and especially F. Fuke, who passed away 2 months after the launch. We thank D. Rowlands for help with modeling the four-way Doppler observable; F. Lemoine for discussions; and T. Arai, H. Takeda, C. K. Shum, and two anonymous reviewers.

Supporting Online Material
www.sciencemag.org/cgi/content/full/323/5916/900/DC1
Materials and Methods
Figs. S1 to S7
Tables S1 and S2
References

3 November 2008; accepted 6 January 2009
10.1126/science.1168029

Long-Lived Volcanism on the Lunar Farside Revealed by SELENE Terrain Camera

Junichi Haruyama,[1]* Makiko Ohtake,[1] Tsuneo Matsunaga,[2] Tomokatsu Morota,[1] Chikatoshi Honda,[1] Yasuhiro Yokota,[1] Masanao Abe,[1] Yoshiko Ogawa,[2] Hideaki Miyamoto,[3] Akira Iwasaki,[4] Carle M. Pieters,[5] Noriaki Asada,[6] Hirohide Demura,[6] Naru Hirata,[6] Junya Terazono,[6] Sho Sasaki,[7] Kazuto Saiki,[8] Atsushi Yamaji,[9] Masaya Torii,[10] Jean-Luc Josset[11]

We determined model ages of mare deposits on the farside of the Moon on the basis of the crater frequency distributions in 10-meter-resolution images obtained by the Terrain Camera on SELENE (Selenological and Engineering Explorer) (Kaguya). Most mare volcanism that formed mare deposits on the lunar farside ceased at ~3.0 billion years ago, suggesting that mare volcanism on the Moon was markedly reduced globally during this period. However, several mare deposits at various locations on the lunar farside also show a much younger age, clustering at ~2.5 billion years ago. These young ages indicate that mare volcanism on the lunar farside lasted longer than was previously considered and may have occurred episodically.

Unraveling the volcanic history of the Moon is essential for understanding the origin and thermal evolution of the Moon. Mare basalts are the most common volcanic features on the Moon. However, absolute dating of mare deposits is nontrivial because it ultimately requires radiogenic dating of samples, and only a limited number of lunar samples returned by Apollo and Luna missions are currently available from a few locations on the near lunar nearside. A second method, measurements of crater size-frequency distribution with the use of remotely acquired images, is widely used to date planetary surfaces from which we do not have sample information. This method is based on the general paradigm that a newly created surface will accumulate craters with time (*1*–*3*). A considerable number of lunar maria have been dated by using image data from Lunar Orbiters and Apollo missions (*4*–*10*); however, precise age determinations of most maria on the farside have not been performed because of the lack of spatially high-resolution images (*5*). Therefore, a systematic, high-resolution mapping of the entire lunar surface, particularly the farside, is one of the primary objectives of the SELENE (Selenological and Engineering Explorer) (Kaguya) mission.

The Terrain Camera (TC) carried on SELENE is a panchromatic push-broom imager with two optical heads (TC1 and TC2) to acquire stereo data for the entire surface of the Moon (*11*). The TC is an optical part of the Lunar Imager/Spectrometer (LISM) (*11*, *12*). The slant angles of TC1 and TC2 are ±15°, relative to the spacecraft flight direction from the nadir vector. Each head has a linear charge-coupled device sensor of 4096 pixels. The instantaneous field of view is 0.00553° and the sampling interval is 6.5 ms, corresponding to 10-m cross- and along-track resolutions, respectively, on the lunar surface at the SELENE nominal altitude of 100 km. The width of the TC swath is 35 km in the normal-swath mode, which provides sufficient overlaps in TC data of sequential observations for producing mosaic images.

SELENE was launched on 14 September 2007 and inserted into a lunar polar orbit on 4 October 2007. Since the beginning of the nominal mission phase on 21 December 2007, the TC has now obtained high-resolution images of most areas of the lunar farside under solar elevation angles lower than ~10°. These images cover previously undated mare deposits on the farside, including those in the South Pole–Aitken (SPA) basin and the Moscoviense basin (e.g., Figs. 1A and 1B are mosaicked images of Antoniadi crater in SPA and Mare Moscoviense, respectively; enlarged figures of Fig. 1, A and B, are shown in figs. S1 and S2).

By using the newly obtained TC data, we performed crater size-frequency distribution measurements for the mare deposits in both SPA and the Moscoviense basin (Table 1). For each region, craters were manually counted using images on computers. Because age determination is sensitive to any contamination by secondary craters (*13*), we excluded areas covered by long shadows from higher terrains and occupied by obvious secondary craters based on their morphological characteristics, such as chain craters, elliptical craters, and clusters (*14*). From these data, absolute model ages of conspicuous mare deposits on the farside of the Moon were obtained. Our results are complimentary to model ages of the nearside mare deposits, which have been studied extensively (*8*–*10*).

We assume that a lunar crate size-frequency distribution (CSFD) can be expressed by the following polynomial for 100 m < D < 200 km proposed by (*2*, *3*, *15*)

$$\log_{10}N(D) = a_0 + \sum_{n=1}^{11} a_n[\log_{10}(D)]^n \quad (1)$$

where D is the crater diameter in kilometers and $N(D)$ is the number of craters with a diameter ≥D per square kilometer. We assigned commonly accepted values for the coefficients of a_1 to a_{11} (*2*, *3*). By fitting an observed CSFD to Eq. 1, we derived the coefficient a_0 [where $a_0 = \log_{10}N(1)$], which gives the age t of the unit in billion years ago (Ga) by using the cratering chronology curve (*2*, *3*, *15*) expressed by

$$N(1) = 5.44 \times 10^{-14}[\exp(6.93 \times t) - 1] + 8.38 \times 10^{-4}t \quad (2)$$

The model ages from crater counts are principally limited by the statistic error (*16*). The quality of the age determination thus improves statistically when the number of countable craters increases and craters are measured over a wide diameter range. In other words, acquisition of images with high spatial resolution and under favorable illumination geometries is crucial, especially for determining model ages of small and/or young areas, where only a few craters are visible in lower-resolution

[1]Institute of Space and Astronautical Science, Japan Aerospace Exploration Agency, 3-1-1 Yoshino-dai, Sagamihara, Kanagawa 229-8510, Japan. [2]Center for Global Environmental Research, National Institute for Environmental Studies, 16-2 Onogawa, Tsukuba, Ibaraki 305-8506, Japan. [3]University Museum, University of Tokyo, 7-3-1 Hongo, Bunkyo-ku, Tokyo 113-0033, Japan. [4]Department of Aerospace and Astronautics, University of Tokyo, 7-3-1 Hongo, Bunkyo-ku, Tokyo 113-8656, Japan. [5]Department of Geological Sciences, Brown University, Providence, RI 02912, USA. [6]University of Aizu, Ikki-machi, Aizu-wakamatsu, Fukushima 965-8580, Japan. [7]RISE Project Office, National Astronomical Observatory of Japan, 2-12 Hoshigaoka, Mizusawa, Oshu 023-0861, Japan. [8]Department of Earth and Space Science, Graduate School of Science, Osaka University, 1-1 Machikaneyama, Toyonaka 560-0043, Osaka, Japan. [9]Division of Earth and Planetary Sciences, Kyoto University, Sakyo-ku, Kyoto 606-8502, Japan. [10]Fujitsu, Chiba 261-8588, Japan. [11]Space Exploration Institute CP 774, CH-2002 Neuchatel, Switzerland.

*To whom correspondence should be addressed. E-mail: haruyama.junichi@jaxa.jp

images. The high-resolution images from the TC that are taken at low sun illumination geometries are particularly suitable for dating small deposits such as those in the SPA basin. The statistical error of individual data points in our crater frequency measurements is mostly <20% (1σ); the errors of ages based on the model (*2*, *3*) are ±0.02 Ga for >3.5 Ga, 0.01 to 0.03 Ga for between 3.2 and 3.0 Ga, and <20% for <3.0 Ga (*8*).

The SPA basin is the largest and deepest impact basin on the Moon: more than 8 km in depth and extending ~2500 km from the south pole to the crater Aitken, which is located 15° south of the equator (*5*). Although a few ancient cryptomaria were observed within the basin (*17*), based on stratigraphical analyses, most mare deposits in the SPA basin were thought to have formed during the late Imbrian epoch (3.85 to 3.8 Ga) (*5*, *18*–*21*). On the basis of our CSFD measurements, we find that most mare deposits are late Imbrian in age (Table 1), consistent with previous stratigraphical work (*5*, *18*, *19*). However, several mare deposits show younger model ages up to Eratosthenian. For example, in the 143-km diameter Antoniadi crater (70°S, 172°E), there is an apparently smooth, young-looking mare deposit (Fig. 1A), which is the southernmost mare deposit in the SPA basin. The derived model age of this deposit is as young as 2.58 Ga (Fig. 2A); hence, it is substantially younger than the Imbrian-Eratosthenian boundary (3.2 Ga).

For several mare deposits, we can fit multiple production function curves to our CSFD, similar to observations of some maria on the nearside (*22*). Apollo N, the easternmost mare deposit in the SPA basin, which has been previously classified as late Imbrian in age (*5*, *7*, *18*), is used as an example. The CSFD (Fig. 2B) for craters larger than 700 m in diameter gives a 3.51-Ga model age of the deposit, which is consistent with previous interpretations (*7*). However, when we assess craters <500 m in diameter by taking advantage of the TC's high-resolution, we derive a second model age of 2.49 Ga (Fig. 2B). It is difficult for this distribution to be generated by adding only a CSFD from an acceptable power-law distribution of secondary craters. A reasonable interpretation for the two distinct model ages is that Apollo N basalts have been formed by multiple eruptions, as observed for several maria on the nearside, including those in Oceanus Procellarum, Imbrium, and Tranquillitatis (*22*). In our interpretation, this Apollo N area has been resurfaced by a basaltic eruption at ~2.5 Ga, where the erupted lava did not completely obliterate preexisting craters on a deposit formed at ~3.5 Ga. The data suggest the size of obliterated craters is less than several hundred meters. Thus, if we consider that the diameter–to–rim-height ratio of a typical lunar crater of <1 km is <0.05 (*23*), the thickness of the younger deposit can be estimated as <40 m.

Mare Moscoviense fills a part of the 550-km diameter Moscoviense basin (27°N, 146°E) (Fig. 1B), which is in the northern hemisphere of the lunar farside. Within the mare, three units have been identified on the basis of color difference in the Clementine ultraviolet-visible multispectral images: (i) an oldest basaltic unit with low estimated FeO content in the southern part, (ii) a northwestern basaltic unit with low TiO_2 content, and (iii) an eastern younger unit with higher TiO_2 content (*24*). The southern unit appeared to be saturated for craters smaller than several hundred meters in diameter. Whereas the CSFD of the northwestern unit reveals a model age of 3.50 Ga, the eastern unit is younger and has a model age of 2.57 Ga (Fig. 2C). The model age of the eastern unit for craters larger than 1 km is close to that of the northwestern unit, which we interpret to indicate that the eastern unit is superposed on an older unit of 3.50 Ga in age. Because of their

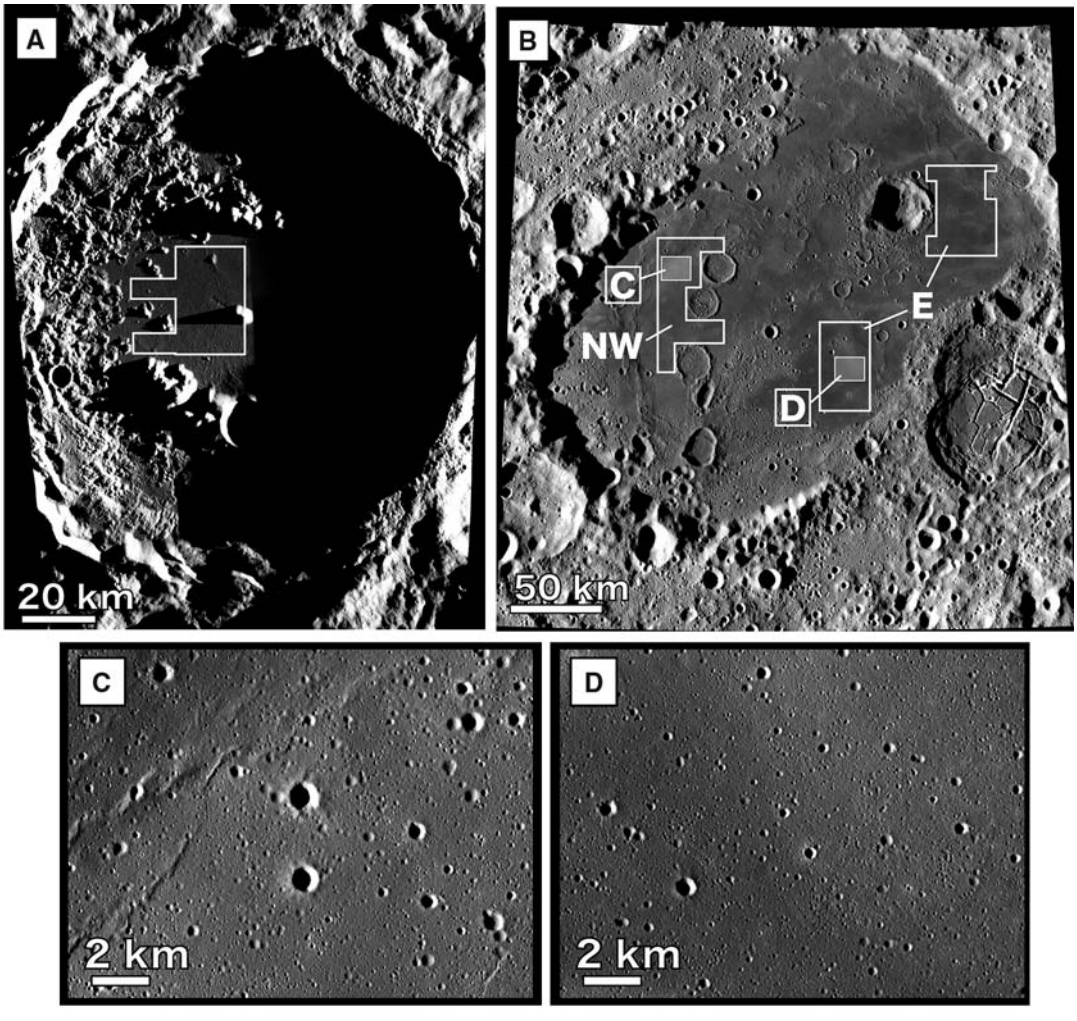

Fig. 1. Mosaics of TC images. (**A**) Antoniadi crater, which shows a dark and smooth mare deposit on its floor. Crater counting was performed for the area outlined by the white polygon. (**B**) Mare Moscoviense, which is filled with mare deposits within its 210-km-diameter inner ring. Crater counting was performed for areas outlined by the white polygons (Table 1). E and NW denote the eastern and northwestern areas, respectively. (**C** and **D**) Close-up images of the mare deposits in Mare Moscoviense. The locations of these deposits are shown as hatched gray boxes in (B). These images are Transverse Mercator map projections.

similar model ages, we propose that the eastern (later) basaltic eruption might have spread over parts of the northwestern unit but did not completely obliterate the previously formed craters on the underlying northwestern unit. We estimated the younger, uppermost unit is 30 to 50 m thick. Several other deposits on the farside show similar characteristics to those in Apollo N and Mare Moscoviense, indicating a potentially complex history of these farside deposits.

Frequency distributions of all estimated ages for maria on the lunar farside (Fig. 3A) from both our study (black bars) and previous studies (gray bars) (*6*–*8*) indicate that most mare units on the lunar farside formed before 3.0 Ga. Because most mare on the nearside are also older than ~3.0 Ga (*8*–*10*) (Fig. 3B), it appears that the global volcanic activity on the Moon declined markedly after 3.0 Ga. However, it is notable that some mare units on the farside show younger model ages clustered around 2.5 Ga (Fig. 3A). Basaltic volcanism also continued on the nearside, but in contrast, the youngest model ages of basaltic unit extend to nearly 1.0 Ga in Oceanus Procellarum.

The global cessation of most lunar mare volcanism by ~3.0 Ga suggests a similar early lunar thermal history for the nearside and farside. Thus, the internal structure of the Moon and its cooling and/or heating during this early period appear to be controlled by the same constraints on a global scale. In combination with previous CSFD analyses (*9*), our results indicate that the timing of the termination of mare basalt volcanism differs between the farside (2.5 Ga) and the nearside (1.2 Ga). This difference might be related to a larger crustal thickness on the lunar farside, which makes it harder for magma to reach the surface (*25*), and/or a deficiency of heat-producing radiogenic elements on the farside as compared with the nearside (*26*). It should be noted that the young mare deposits are widespread throughout the farside, from the Moscoviense basin in the

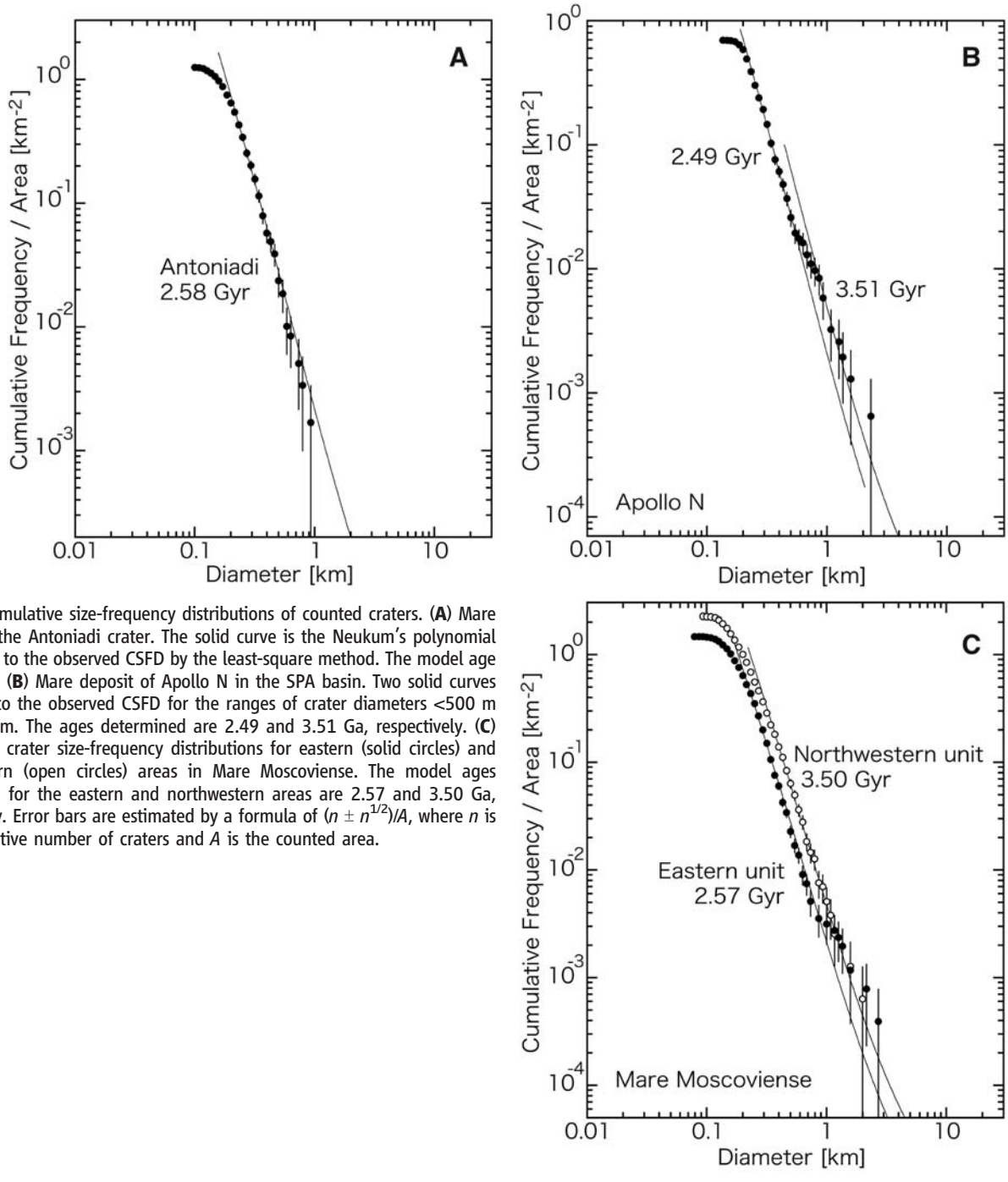

Fig. 2. Cumulative size-frequency distributions of counted craters. (**A**) Mare deposit in the Antoniadi crater. The solid curve is the Neukum's polynomial function fit to the observed CSFD by the least-square method. The model age is 2.58 Ga. (**B**) Mare deposit of Apollo N in the SPA basin. Two solid curves can be fit to the observed CSFD for the ranges of crater diameters <500 m and >700 m. The ages determined are 2.49 and 3.51 Ga, respectively. (**C**) Cumulative crater size-frequency distributions for eastern (solid circles) and northwestern (open circles) areas in Mare Moscoviense. The model ages determined for the eastern and northwestern areas are 2.57 and 3.50 Ga, respectively. Error bars are estimated by a formula of $(n \pm n^{1/2})/A$, where n is the cumulative number of craters and A is the counted area.

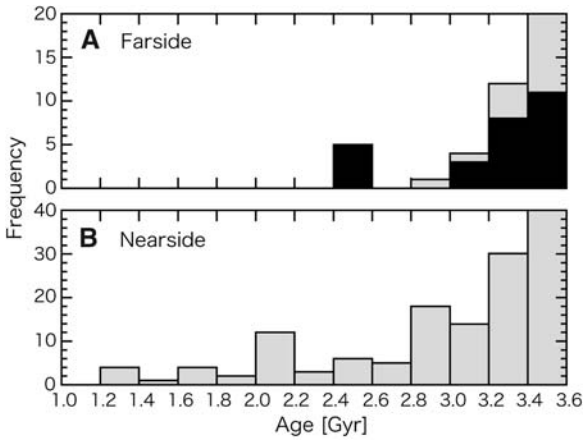

Fig. 3. Histograms of the model ages of mare deposits on the farside (**A**), including those in Mare Moscoviense, the SPA basin, Tsiolkovsky (*6*), Mare Orientale (*7*), and Mare Australe (*8*), and on the nearside (**B**), including those in Mare Imbrium, Serenitatis, Humorum, Tranquillitatis, Humboldtianum (*8*), Oceanus Procellarum, Mare Nubium, Cognitum, Insularum (*9*), and Mare Fecunditatis (*10*). Black bars indicate mare deposits, whose ages are newly determined by this study.

Table 1. Model ages for maria on the lunar farside.

Mare		Area (km^2)	SEA* (degrees)	$N(1)$† (km^{-2})	Age (Ga)	Previous studies‡
Poincare	S	734.0	2.1	0.00284	3.17	Im (*5*)
	NW	490.6	2.0	0.00433	3.46	Im (*5*)
	E	1067.2	2.5	0.00277	3.13	Im (*5*)
				0.00504	3.52	
Ingenii		1291.8	9.9	0.00292	3.20	Im (*5, 18*)
				0.00489	3.51	
Antoniadi		592.7	2.8	0.00217	2.58	Im (*5*); EIm (*19*)
Chretien		1183.1	2.3	0.00315	3.28	Im (*5, 18*)
				0.00427	3.46	
Jules Verne		815.2	11.1	0.00343	3.34	Im (*5, 18*)
Aitken		1257.1	10.9	0.00315	3.28	Im (*5, 18*); 3.8 Ga (*4*)
				0.00469	3.49	
Apollo N		1541.5	5.5	0.00209	2.49	Im (*5, 18*), 3.63 Ga (*7*)
				0.00491	3.51	
Apollo S		778.4	5.1	0.00205	2.44	Im (*5, 18*), 3.63 Ga (*7*)
Von Karman		1628.6	3.0	0.00349	3.35	Im (*5, 18*)
Von Karman M		1220.6	2.9	0.00364	3.38	Im (*5, 18*)
Leibnitz		926.0	3.6	0.00410	3.44	Im (*5, 18*)
				0.00473	3.50	
Rumford		239.0	4.5	0.00346	3.35	Im (*5, 18*)
Maksutov		615.3	4.3	0.00311	3.27	Im (*5, 18*)
				0.00451	3.48	
Nishina		596.7	4.1	0.00207	2.47	Im (*5*)
				0.00282	3.16	
				0.02406	3.85	
Moscoviense	NW	1576.1	11	0.00481	3.50	Im (*5, 18*)
	E	2543.5	11	0.00216	2.57	Im (*5, 18*)
				0.00562	3.55	

*Solar elevation angle (SEA) of image used for crater counting. †$N(1)$ is the number of craters with a diameter larger than or equal to 1 km per km^2, derived by fitting a polynomial proposed in (*2*, *3*) to observed CSFDs. ‡Im, Imbrian mare materials; EIm, Eratosthenian–Imbrian mare materials.

north to within the Antoniadi crater in the south. In addition, our data suggest these young basalts might have erupted during a late pulse of volcanic activities on the lunar farside near ~2.5 Ga. Alternatively, the lack of observed farside volcanism between 2.5 and 3.0 Ga might merely be explained by continuous superposition of younger deposits.

References and Notes

1. W. K. Hartmann, *Icarus* **5**, 406 (1966).
2. G. Neukum, *Meteoritenbombardment und Datierung Planetarer Oberflächen* (Ludwig Maximilians Univ., Munich, Germany, 1983).
3. G. Neukum, B. A. Ivanov, in *Hazards Due to Comets and Asteroids*, T. Gehrels, Ed. (Univ. of Arizona Press, Tucson, AZ, 1994), pp. 359–415.
4. A. S. Walker, F. El-Baz, *Moon Planets* **27**, 91 (1982).
5. D. E. Wilhelms, *The Geologic History of the Moon. U.S. Geological Survey Professional Paper* (U.S. Geological Survey, Washington, DC, 1987).
6. A. Tyrie, *Earth Moon Planets* **42**, 245 (1988).
7. R. Greeley *et al.*, *J. Geophys. Res.* **98**, 17183 (1993).
8. H. Hiesinger, R. Jaumann, G. Neukum, J. W. Head III, *J. Geophys. Res.* **105**, 29239 (2000).
9. H. Hiesinger *et al.*, *J. Geophys. Res.* **108**, 5065 (2003).
10. H. Hiesinger *et al.*, *37th Lunar Planet. Sci. Conf.*, no. 1151 (2006).
11. J. Haruyama *et al.*, *Earth Planets Space* **60**, 243 (2008).
12. LISM consists of the TC, Multi-Band Imager (MI), and Spectral Profiler (SP). MI is a multicolor imager with nine bands in the visible–to–near-infrared range, and SP is a continuous spectral profiling sensor in the same range. See (*11*) for LISM's specifications and operation strategy.
13. A. S. McEwen, E. B. Bierhaus, *Annu. Rev. Earth Planet. Sci.* **34**, 535 (2006).
14. H. J. Melosh, *Impact Cratering: A Geologic Process* (Oxford Univ. Press, New York, 1989).
15. We investigated model dependencies of adopted functions (Eqs. 1 and 2), as compared with two other well-established models. A lunar CSFD function model suggested by Hartmann (*27*), that includes three power laws for different diameter ranges, would yield different model ages over a wide range of crater diameters (*16*, *28*). However, in the diameter range we use (a few kilometers to a few hundred meters), the difference between the functions is <10% (*28*), which gives small differences in the estimated ages. More recently, a different chronology curve between age and number of craters was proposed (*29*). The newer model shows a steeper slope in the age range of >3.75 Ga, where the difference from the model we adopt becomes large. However, in the range of <3.6 Ga, ages from the newer model would differ less than 0.1 Ga from our results.
16. G. Neukum, B. A. Ivanov, W. K. Hartmann, *Space Sci. Rev.* **96**, 55 (2001).
17. C. M. Pieters, L. Gaddis, B. Jolliff, M. Duke, *J. Geophys. Res.* **106**, 28001 (2001).
18. D. E. Stuart-Alexander, *U.S. Geol. Surv. Map I-1047* (1978).
19. D. E. Wilhelms, K. A. Howard, H. G. Wilshire, *U.S. Geol. Surv. Map I-1162* (1979).
20. The lunar geologic periods are divided into pre-Nectarian (from 4.2 to 3.92 Ga), Nectarian (from 3.92 to 3.85 Ga), early Imbrian (from 3.85 to 3.8 Ga), late Imbrian (from 3.8 to 3.2 Ga), Eratosthenian (from 3.2 to 1.1 Ga), and Copernican (from 1.1 Ga to the present) (*5*).
21. Although a detailed documentation of farside cryptomaria is beyond the scope of this discussion, the role of these ancient basalts in early phases of lunar volcanism will become better defined as additional remote sensing data for the Moon are returned.
22. H. Hiesinger *et al.*, *Geophys. Res. Lett.* **29**, 1248 (2002).
23. R. J. Pike, in *Impact and Explosion Cratering*, D. J. Roddy, R. O. Pepin, R. B. Merrill, Eds. (Pergamon, New York, 1977), pp. 489–510.
24. G. Y. Kramer, B. L. Jolliff, C. R. Neal, *J. Geophys. Res.* **113**, E01002 (2008).
25. J. W. Head III, L. Wilson, *Geochim. Cosmochim. Acta* **56**, 2155 (1992).
26. B. L. Jolliff *et al.*, *J. Geophys. Res.* **105**, 4197 (2000).
27. W. K. Hartmann, *Meteorit. Planet. Sci.* **34**, 167 (1999).
28. B. A. Ivanov, *Space Sci. Rev.* **96**, 87 (2001).
29. D. Stöffler, G. Ryder, *Space Sci. Rev.* **96**, 9 (2001).

30. We thank all the contributors to the SELENE (Kaguya) project, especially members of the project management group (Y. Takizawa, M. Kato, S. Sasaki, R. Nagashima, K. Tsuruda, and H. Mizutani) and the Lunar Imager/Spectrometer working group (H. Otake, H. Kawasaki, R. Nakamura, S. Kodama, S. Minami, S. Takechi, A. Akiyama, M. Shirao, T. Yokota, H. Takeda, T. Arai, T. Sugihara, Y. Yamaguchi, T. Hiroi, T. Hashimoto, T. Michikami, K. Kitazato, M. Higa, P. Pinet, T. Nimura, T. Yamamoto, N. Harada, K. Iseki, T. Hodokuma, S. Kikuchi, S. Kawabe, S. Okuno, and T. Takayama), for their efforts in development, operation, and data processing of SELENE and LISM/TC. We also thank the three anonymous reviewers for their helpful comments. This work was supported by KAKENHI (grant 20540416 to J.H. and C.H.), (19204045 to H.D.), and (20•9211 to T.M.).

Supporting Online Material

www.sciencemag.org/cgi/content/full/1163382/DC1
SOM Text
Figs. S1 and S2
Table S1

17 July 2008; accepted 30 September 2008
Published online 6 November 2008;
10.1126/science.1163382
Include this information when citing this paper.